Menthol reduces phototoxicity pain in a mouse model of photodynamic therapy

Wright, Lisa; Baptista-Hon, Daniel; Bull, Fiona; Dalgaty, Faith; Gallacher, Michael; Woods, Julie A.; Ibbotson, Sally H.; Hales, Tim G.

Published in:
Pain

DOI:
10.1097/j.pain.0000000000001096

Publication date:
2018

Document Version
Peer reviewed version

Menthol reduces phototoxicity pain in a mouse model of photodynamic therapy

Lisa Wright[1], Daniel Baptista-Hon[1], Fiona Bull[1], Faith Dalgaty[1], Michael Gallacher[1], Julie A. Woods[2], Sally H. Ibbotson[2] and Tim G. Hales[1]

[1]The Institute of Academic Anaesthesia, Division of Neuroscience, Medical research Institute and [2]The Photobiology Unit, Ninewells Hospital, University of Dundee, Dundee, DD1 9SY, UK

Address correspondence to: Tim G. Hales, The Institute of Academic Anaesthesia, Division of Neuroscience, Medical research Institute, Ninewells Hospital, University of Dundee, Dundee, DD1 9SY, UK. Phone: +44 (0)1382 383443; Email: t.g.hales@dundee.ac.uk .

Running title: Menthol reduces PDT pain in mice

Number of text pages: 30

Number of figures: 7

Number of tables: 0

Key Words: Phototoxicity; photosensitisation; porphyria; reactive oxygen species; electrophysiology; behavioral neuroscience

Abstract

Phototoxicity-induced pain is a major clinical problem triggered by light acting on photosensitising drugs or endogenous porphyrins, notably protoporphyrin IX (PpIX), an intermediary in heme biosynthesis. PpIX accumulates in individuals with erythropoietic protoporphyria and is elevated during photodynamic therapy subsequent to application of 5-aminolevulinic acid (ALA). Pain occurs during irradiation of PpIX and responds poorly to conventional analgesics. Our objective was to develop a model of PpIX phototoxicity pain and investigate the potential of menthol as an analgesic. Application of ALA to the tails of C57 black and SWISS white mice caused PpIX accumulation and nociception during irradiation (630 nm at 3.7 J/cm^2). Despite similar PpIX accumulation, C57 mice exhibited less pain behavior compared to SWISS mice due to light absorption by pigmentation. Irradiation of ALA-treated dorsal root ganglion neurons caused phototoxicity-evoked action potentials (APs) in both mouse strains. The antioxidant L-tryptophan increased the light dose required to elicit such APs. By contrast, the addition of keratinocytes to neuronal cultures decreased the threshold for APs, suggesting a requirement for proliferating cells. Inhibition of fatty acid amide hydrolase, selective antagonism of TRPV1 or the application of lidocaine or its quaternary derivative QX-314, reduced AP frequency, while antagonism of TRPA1 had no effect. These results suggest that products of singlet O_2-mediated lipid peroxidation trigger nociceptor activation via TRPV1. Menthol inhibited phototoxicity-evoked APs and reduced pain behavior when applied topically to mice. These findings suggest that menthol might provide pain relief in patients experiencing PpIX-phototoxicity pain caused by photodynamic therapy or erythropoietic protoporphyria.

1. Introduction

Phototoxicity is relatively common in patients prescribed photoactive drugs and is the basis for photodynamic therapy (PDT) [19,27,28,38]. Phototoxicity also occurs in the light-exposed skin of patients suffering from erythropoietic protoporphyria (EPP) in whom the photoactive molecule protoporphyrin IX (PpIX) accumulates [18,36]. When exposed to light, fluorescent molecules generate reactive singlet oxygen ($^1O_2$) from triplet oxygen by a type two reaction and free radicals, such as superoxide, by a type one reaction [12]. Endogenous antioxidants help overcome cellular damage, but this protection is overwhelmed during phototoxicity leading to cell death [22].

PpIX accumulation is normally restricted by the rate-limiting step at aminolevulinic acid (ALA) synthase, a mitochondrial enzyme within the heme pathway and ferrochelatase, which rapidly inserts ferrous iron into PpIX thereby limiting its phototoxic potential. Autosomal recessive loss-of-function mutations in the ferrochelatase gene, usually in combination with a low-expressing polymorphic allele, lead to the most common erythropoietic protoporphyria [2]. Protoporphyria can also be caused by rare gain-of-function mutations in the erythroid-specific ALA synthase gene [13].

PpIX-phototoxicity is exploited therapeutically in the controlled delivery of topical PDT to treat non-melanoma skin cancers, such as basal cell carcinoma (BCC), pre-cancers and other diverse skin diseases including actinic keratosis (AK) [27,28]. PpIX accumulates following application of a pro-drug, such as ALA. The generation of $^1O_2$ during irradiation destroys diseased tissue. However, a burning sensation typically occurs and pain is the most common adverse effect of PDT [19,27,28,38]. Pain can be mild to severe, displaying marked individual variability.

Blue light (405 nm), often used during PDT for superficial AK, effectively photoactivates PpIX. A recent study demonstrated that 405 nm irradiation itself causes pain associated with activation of TRPA1 and TRPV1 channels in dorsal root ganglion (DRG) neurons, which was enhanced by elevated PpIX [1]. Blue light has limited tissue penetration and more deeply penetrating red light (630 nm) is often used as an alternative during PDT. Red light alone does not have any effects, however, in the presence of PpIX-mediated photosensitization, the combination causes pain of unknown mechanism [38].

Approaches for PDT pain management such as light-interruption, topical local anesthetics, oral analgesics and cooling, have had limited success [19,27,28,38]. There is a need for more effective PDT pain relief and experimental models are required in order to develop new approaches.

Despite its known analgesic properties and wide availability, topical menthol has not previously been investigated as a potential means of pain prevention or relief during PDT. There are a number of reasons why menthol might be a good choice. It evokes a cooling sensation through activation of TRPM8 receptors [4]. This might be advantageous as skin cooling causes a small reduction in PDT pain [35]. Furthermore, menthol directly inhibits voltage-activated Na^+ channel activity and increases paw withdrawal latency from noxious heat [21,30].

We developed a mouse model of pain and hyperalgesia evoked by PDT with red light and used DRG neurons to examine the mechanisms involved in PDT phototoxicity-evoked action potentials and the potential role of topical menthol for PpIX phototoxicity pain prevention.

2. Methods

2.1. Cell culture

Dorsal root ganglia were harvested from NIH SWISS and C57BL/6 mice (postnatal day 8 to 10). Cells were dissociated both enzymatically (collagenase/dispase (4 mg/ml) and papain (40 units/ml)) and physically by trituration. Neurons were plated onto poly-D-lysine- and laminin-coated coverslips (13 mm diameter) in the center of 35 mm dishes (VWR, Leicestershire, UK), as described previously [37]. Cells were cultured in Dulbecco's modified Eagle medium (DMEM) / F-12 nutrient mixture (DMEM/F-12), supplemented with heat-inactivated fetal bovine serum (FBS; 10%), nerve growth factor (NGF; 50 ng/ml) and penicillin (100 μg/ml) and streptomycin (100 units/ml) (Pen/Strep) at 37^{o}C and 5% CO_2. DRG cells were maintained in culture for up to 15 days. HaCaT and HEK cells were maintained in DMEM supplemented with FBS (5%), non-essential amino acids (1%) and Pen/Strep at 37^{o}C and 5% CO_2. For combined cultures, HaCaT cells were plated onto the poly-D-lysine- and laminin- coated coverslips on the day preceding DRG dissociation. Harvested DRG cells were plated on HaCaT-cell coated coverslips. Co-cultures were incubated at 37^{o}C and 5% CO_2 for a further 3 days prior to recording. For electrophysiological studies, HEK cells were seeded in 35 mm culture dishes. cDNAs encoding rat TRPV1 receptors (Origene, Rockville, MD, USA) or rat TRPA1 receptors (a gift from Dr Gerard Ahern, Georgetown University) were transfected into HEK cells using calcium phosphate precipitation. Reagents were obtained from Invitrogen (Paisley, UK) or Sigma-Aldrich (Dorset, UK).

2.2. Flow cytometry

Cells were seeded onto 60 mm dishes and incubated in media in the absence or presence of ALA (1 mM; Sigma-Aldrich, Dorset, UK) for 4 h at 37^{o}C and 5% CO_2. Cells were washed with phosphate buffered saline (PBS) and harvested using a non-enzymatic cell dissociation solution (Sigma-Aldrich, Dorset, UK). Following centrifugation at 3000 rpm for 5 min, cells were resuspended in PBS. Fluorescence mediated by PpIX was measured using flow cytometry. 10,000 cells per sample were analyzed on a FACScan flow cytometer, using a 15-mW blue (488 nm) argon laser to excite PpIX. Emitted fluorescence was detected at ≥650nm. Data were acquired using Cell Quest Pro 5.2.1 (Becton Dickinson Immunocytochemistry Systems, California, USA). Analysis was performed using FlowJo 9.7.5 software (www.treestar.com). Regions of interest containing healthy cell populations were identified on the basis of forward and side

light scatter enabling the subsequent production of fluorescence histograms, as described previously [37].

2.3. PpIX Irradiation

For *in vitro* experiments, cells were incubated (4-7 h) in the dark, in media with or without ALA (1 mM). The ALA incubation time is in keeping with the conditions used in patients, where ALA would usually be applied for 3-6 h. Cells were irradiated (20 min) using a diode laser at 630 nm, with an irradiance of 96 mW/cm^2, corresponding to a total light dose of 115.2 J/cm^2. Action potential responses occurred with light doses of $\geq$ 6 J/cm^2 (see Results). For *in vivo* studies, 630-nm laser irradiation lasted 60 s, with an irradiance of 62 mW/cm^2, corresponding to a light dose of 3.7 J/cm^2. The light dose required to produce reliable pain behaviour in SWISS mice was determined empirically. The light doses are within the range used clinically during PDT [14].

2.4. Electrophysiology

The patch-clamp technique was used to record whole-cell, and outside-out or cell-attached patch currents (voltage-clamped at 0 and -60 mV, respectively), and action potentials (current-clamp). Borosilicate glass recording electrodes when filled with intracellular solution had resistances of 1.8 - 3 MΩ. For excised patch recordings the electrode solution contained (in mM): 140 CsCl, 2 $MgCl_2$, 11 EGTA, 3 Mg-ATP, and 10 HEPES (pH 7.4 with CsOH). The extracellular solution contained (in mM): 140 NaCl, 4.7 KCl, 1.2 MgCl2, 2.5 CaCl2, 10 glucose and 10 HEPES (pH 7.4 with NaOH). The extracellular solution was used within the electrode during cell-attached recordings. Current-clamp recordings utilized an electrode solution containing (in mM): 140 potassium gluconate, 10 NaCl, 2.8 KCl, 2 $MgCl_2$, 0.1 $CaCl_2$, 1.1 EGTA and 10 HEPES (pH 7.4 with KOH). The extracellular solution was the same as that used in voltage-clamp recordings. Current-clamp data were corrected for the calculated liquid junction potential. Electrophysiological recordings were performed under subdued lighting. The diode laser was used to examine the effects of irradiation under control conditions or following incubation with ALA (1 mM). All electrophysiological data were recorded using an Axopatch 200A amplifier (Molecular Devices, CA, USA). Data were low pass filtered at 2 kHz, digitised at 8 kHz using a Digidata 1322A interface, acquired and analysed using pClamp 10.2 software (from Molecular Devices). Action potentials were detected by the threshold method and verified by visual inspection. Instantaneous action potential frequencies were determined and bursts were defined as >5 consecutive events with an instantaneous frequency >0.1 Hz. The latency to

response was determined as the time taken for irradiation to generate a burst of action potentials. The frequency of action potentials was determined during the entire 1200 s irradiation.

2.5. Cell viability assay

Viability was assessed using 3-(4,5-dimethyl-2-thiazolyl)-2,5-diphenyl-2H-tetrazolium bromide (MTT). Control or PDT treated cells were incubated (2 h) in media containing 0.6 mg/ml MTT. Cells were washed with PBS and images digitally captured using a Moticam 2500 camera with Motic Images Plus 2.0 software (Microscopy Supplies and Consultants Ltd, Fife, UK).

2.6. Confocal imaging

Experiments were performed in the Light Microscopy Core Facility. PpIX fluorescence was visualised in DRG neuronal cultures using confocal microscopy. DRG cultures were treated with ALA (1 mM for 4 h). Cells were then examined under a Leica TCS SP-5 confocal microscope (Leica, Newcastle, UK) at 40x magnification in DMEM lacking phenol red. PpIX was excited at 405 nm and the emitted fluorescence was collected between 610 and 650 nm.

2.7. Behavioral Studies

Mice were bred, maintained and housed in the Ninewells Hospital Medical Resource Unit in accordance with the University of Dundee's Ethics Committee and UK Home Office regulations, with an appropriate project license. They had access to food and water *ad libitum* with 12 hour cycles of light and dark, the temperature was maintained between 19 and 21°C. All experiments were performed in the light phase. Studies were performed in the Behavioural Neuroscience Core Facility. NIH SWISS and C57BL/6 mice were habituated to handling 3 days prior to the commencement of behavioral studies. Soft white paraffin (50 mg; vehicle) or ALA (20% w/w; Mandeville Medicines, Buckinghamshire, UK) cream was applied to tails. Mice were kept in darkness for 4 h prior to irradiation and behavioral studies were conducted under subdued lighting. As described previously [20], laser diode fluorescence spectroscopy was used to confirm the conversion of ALA uptake to PpIX. Light at a wavelength of 405 nm was used to excite PpIX within mouse tails. Emitted fluorescence was acquired onto a PC for analysis (LabVIEW software, National Instruments, London, UK). PpIX-mediated fluorescence was detected between 600-750 nm, with peak fluorescence at 634 nm. Measurements from human forearm were performed alongside mouse measurements for comparison. In some cases mouse

PpIX fluorescence was normalised to that of human PpIX fluorescence acquired on the same day (expressed as % fluorescent units (FU)). Tails were exposed to light emitted from a diode laser (630 nm, irradiance 62 mW/cm^2, 60 s, light dose 3.72 J/cm^2), in order to assay PpIX phototoxicity pain. Pain behavior was assayed by measuring the time spent tail lifting, holding and licking the tail within 60 s following laser exposure. Experiments examining the potential analgesic action of menthol were blinded. In order to habituate animals and investigators to menthol odour, a vapour source was present throughout the period of these experiments. Aqueous cream (0.4 g) or menthol (2% or 16%) was applied to tails 10 min prior to irradiation. For studies examining tail withdrawal latencies tails were exposed to temperatures ranging from 37 – 53^{o}C.

2.8. Temperature measurements

The laser-induced temperature increase within the recording chamber was determined using a digital thermo-hygrometer (VWR, Leighton Buzzard, UK). The temperature was recorded every 30 s for the duration of irradiation. An infrared thermoIMAGER 160 camera and TIM Connect software (Micro-Epsilon UK Ltd, Birkenhead, UK) were used to determine the effect of laser irradiation on mouse tail temperature recorded continuously over a period of 60 s.

2.9. Statistical analysis

Data are represented as mean ± standard error of mean (SEM). Statistical analyses were performed using IBM SPSS 22. Analyses of tail withdrawal data were performed using the Wilcoxon signed rank test or the Kruskall Wallis test. Other pairwise analyses of means were performed using the t-test. One-way or two-way ANOVA were used to analyse multiple groups, as appropriate. Multiple comparison corrections were performed using either Dunnett's or Tukey's correction for one-way ANOVA, or Bonferroni's correction for two-way ANOVA. Correlation between PpIX emission and pain behaviour was performed using a Pearson correlation test. Exact p values are reported where possible (except when $p < 0.0001$) and data were considered statistically significant when $p < 0.05$.

2.10. Drug application

For *in vitro* experiments, drugs, made fresh from stocks on the day of experimentation, were applied either to the bath prior to irradiation (AMG-9810, HOE140, AA-5-HT, PF-3845, lidocaine, QX-314 and menthol), or focally by pressure ejection (PicoSpritzer II, General Valve Corp., Fairfield, NJ, USA) from a glass micropipette (capsaicin and QX-314). Drug application to outside

out patches of HEK cells containing TRPV1 receptors was achieved using the three-pipe Perfusion Fast-Step system (Warner Instruments, CA, USA), as described previously [3]. Menthol cream (2% and 16%) was made fresh on the day of experimentation. Menthol was dissolved in ethanol (100%) before mixing into aqueous cream. The vehicle consisted of the equivalent volume of ethanol mixed into aqueous cream.

3. Results

3.1. PDT-induced pain behavior in mice

We examined the effect of laser irradiation (630 nm, 3.7 J/cm^2) and ALA applied topically (4-6 h) on the tails of NIH SWISS white mice and C57BL/6 black mice. Neither topical ALA (SWISS; n = 35; C57; n = 17; data not shown), nor laser irradiation alone (SWISS; n = 30; C57; n = 10), caused discernible pain behaviour (see Methods) in either mouse strain (Fig. 1A). The average duration of pain behavior increased from 0.4 ± 0.2 s (n = 30) in vehicle treated SWISS mice to 20 ± 3 s (n = 30) in ALA treated mice during 60 s following laser irradiation of their ALA treated tails (Fig. 1A). Following ALA and laser irradiation, 5 of 10 C57 mice also displayed pain behaviour. The duration of pain behaviour increased from none in vehicle treated C57 mice (n = 10) to 4 ± 2 s (n = 10) in ALA treated mice. In both strains pain behavior ceased within 5 minutes suggesting that the underlying pain was acute and transient.

We compared the influence of ALA and vehicle treatment on laser irradiated tails between SWISS and C57 mice using a two-way ANOVA. The analysis revealed a significant difference in both tail treatment (vehicle vs ALA; $F_{1,76} = 22.1$; $p < 0.0001$) as well as the strain of mouse (SWISS vs C57; $F_{1,76} = 11.2$; $p = 0.001$) on pain behavior. There was also a statistically significant interaction between tail treatment and mouse strain ($F_{1,76} = 10.2$; $p = 0.002$). This suggests that the increase in duration of pain behavior following ALA and laser treatment differed depending on the strain of mouse used. A simple effects comparison using the Bonferroni correction revealed that the pain behavior exhibited by SWISS mice was significantly ($p < 0.0001$) more prolonged than that of C57 mice following treatment with ALA (Fig. 1A). Therefore the data suggest that SWISS mice are more susceptible to PDT-induced pain.

3.2. Pigmentation reduces PpIX-mediated fluorescence and associated pain

We observed PpIX emission non-invasively using fluorescence spectroscopy with fibre-optic coupled laser excitation at 405 nm (Fig. 1B). Compared to vehicle treated control mouse tails, the characteristic PpIX emission spectrum was enhanced by ALA treatment to levels similar to those achieved in the ALA treated human forearm (Fig. 1B). We quantified PpIX emission by measuring the peak fluorescence at 634 nm (see Methods) and normalising this value to that measured from a human forearm (as % control fluorescence units; FU). PpIX emission was evident in the ALA treated tails of both C57 and SWISS mice, following laser irradiation (Fig. 1C). By contrast, mice treated with vehicle exhibited negligible PpIX emission (Fig. 1C). Both C57

mice and SWISS mouse tails showed increased PpIX emission following ALA treatment. However, similar to the pain behavior data (Fig. 1A), PpIX fluorescence emission from ALA treated tails of C57 mice was less (only ~25%) compared to SWISS mouse tails (Fig. 1C). We therefore analysed the PpIX fluorescence emission data using a two-way ANOVA. Our analysis revealed, like the pain behaviour above, that both treatment ($F_{1,100}$ = 56.8) and mouse strain ($F_{1,100}$ = 23.2) significantly influenced PpIX emission ($p < 0.0001$ for both). We also found a significant interaction between tail treatment and mouse strain ($F_{1,100}$ = 19.1; $p < 0.0001$). This suggests that the increase in PpIX emission differs following ALA and laser treatment, depending on mouse strain. Indeed, a simple effects comparison with a Bonferroni correction revealed the difference in PpIX emission between the tails of SWISS and C57 mice to be significant ($p < 0.0001$), following ALA treatment (Fig. 1C). Irradiation using a Wood's lamp also revealed greater visible fluorescence emission from ALA treated tails of SWISS mice compared to those of C57 mice (Supplemental Fig. 1). In addition to the tails, fluorescence was observed in the paws, noses and ears of both mouse strains indicating the systemic accumulation of PpIX.

Pigmentation in C57 mice may absorb irradiation leading to reduced PpIX fluorescence. This could account for the lower level of PpIX-irradiation pain (Fig. 1A). Pigmentation is greatest in the ears and tails of C57 mice, with lower levels in their paws. We therefore compared PpIX emission for each of these tissues following treatment of tails with ALA in C57 and SWISS mice. Consistent with a role for pigmentation in the diminished PpIX fluorescence of C57 tails, we found a significant ($p = 0.006$; t-test) difference in PpIX emission from the ears between C57 and SWISS mice, in which visual inspection revealed a clear difference in pigmentation (Supplemental Fig. 1), but no significant difference ($p = 0.12$; t-test) in the paws, in which neither strain exhibited obvious pigmentation (Fig. 1D). We further explored a role for pigmentation in PpIX emission, by applying black ink to the tails of SWISS mice. We compared PpIX emission from ALA treated tails from C57, SWISS and black ink stained SWISS mice tails. A one-way ANOVA revealed a significant difference ($F_{2,12}$ = 82.7; $p < 0.0001$) between PpIX emission (Fig. 1D). A *post-hoc* Dunnett's comparison showed that both C57 mice tails, and black ink stained SWISS mice tails had significantly lower ($p < 0.0001$) PpIX emission than control SWISS mice tails (Fig. 1D). Taken together our data are consistent with the hypothesis that pigmentation absorbs irradiation, leading to lower PpIX fluorescence emission and, in turn, less pain behavior (Fig. 1A).

The *in vivo* data demonstrate that neither PpIX production nor 630-nm irradiation alone is sufficient to generate pain in mice. By contrast, PpIX fluorescence evoked by irradiation was associated with quantifiable pain behavior. Although PpIX fluorescence was required for pain behavior, there was no correlation ($p = 0.95$; Pearson r coefficient = 0.013) between the level of PpIX fluorescence emission and the extent of pain behavior (Fig. 1E). Having established that SWISS mice exhibited robust PDT pain following ALA treatment, subsequent behavioral experiments were performed using this approach.

3.3. PpIX phototoxicity causes thermal hyperalgesia

PpIX phototoxicity pain in humans is described as a burning sensation implicating sensitisation or activation of thermal nociceptive pathways [19,27,28,38]. We explored this by investigating the effect of PpIX irradiation on subsequent tail withdrawal from heated water. Baseline thermal withdrawal latencies were established by tail immersion in water heated to between 37^{o}C and 53^{o}C (Supplementary Fig. 2). At 53^{o}C the average tail withdrawal latency was 6 ± 2 s (n = 15), with 14 of 15 mice withdrawing within less than 30 s. An intermediate tail withdrawal latency of 24 ± 2 s (n = 15) occurred with water at 48^{o}C, with 9 of 15 mice withdrawing in <30 s. This temperature was chosen to examine the effects of PpIX irradiation on thermal sensitivity. We subsequently examined the tail withdrawal latencies of mice treated with vehicle cream with laser irradiation, ALA cream without laser irradiation and ALA cream with laser irradiation. The mean tail withdrawal latencies are summarised in Figure 1F. A Kruskall-Wallis test revealed significant ($p = 0.018$) differences in tail withdrawal latencies (Fig. 1F). P*ost-hoc* comparisons revealed significant ($p = 0.029$) reduction in tail withdrawal latency in mice exposed to both ALA cream and laser irradiation versus those exposed to vehicle cream and laser (Fig. 1F). 10 of 15 mice responded in this group. No changes in tail withdrawal latencies were observed in mice exposed to irradiation only (n = 15), or ALA cream only (n = 5; Fig. 1F). A PDT-induced reduction in withdrawal latency, without an obvious change in the proportion of mice responding, is consistent with a heightened thermal pain response (hyperalgesia).

3.4. PpIX phototoxicity evokes action potentials in DRG neurons

Primary afferent neurons within dorsal root ganglia (DRG) transmit nociceptive pain from peripheral sites, such as the tail, to the spinal cord. Confocal images of DRG cultures reveal PpIX mediated fluorescence in cells after ALA (1 mM) treatment for 4 h (Fig. 2A). Flow cytometry using dissociated DRG cultures revealed that cells treated with ALA (1 mM for 4 h) produced

PpIX fluorescence emission that was not seen in untreated cells (Fig. 2A). These data demonstrate that ALA, when applied directly, leads to the production of PpIX in DRG cultures. We examined responses of small DRG neurons (<25 μm) to ALA either alone or in combination with laser irradiation (630 nm) using the cell attached configuration to monitor action potentials. This approach preserves the intracellular milieu while action potentials are monitored as a combination of resistive and capacitive currents [15]. Spontaneous action potentials occurred very rarely in recordings from SWISS and C57 DRG neurons (grown for 1-15 days *in vitro*) under control conditions or in recordings from neurons exposed to ALA (1 mM, 4-7 h) prior to irradiation (Fig. 2B, C). By contrast, during laser irradiation (630 nm) neurons from both mouse strains exposed to ALA exhibited bursts of frequent action potentials (Fig. 2B, C). DRG neurons from SWISS and C57 mice exhibited similar responses to PpIX irradiation. Subsequent *in vitro* experiments were performed using DRG neurons from C57 mice.

While 97% of neurons responded to PpIX irradiation (day 4-15 *in vitro*), there was considerable variability in the latency to the first burst of action potentials (486 ± 20 s; n = 135), which equates to a mean light dose of 47 ± 2 J/cm^2 required to evoke a response during the 1200 s laser exposure (total light dose = 115 J/cm^2). The instantaneous frequency of action potentials was 11.6 ± 1.3 Hz (day 7 *in vitro*). The mean frequency of firing during the entire period of irradiation was 0.23 ± 0.03 Hz. Interestingly, despite the known cellular toxicity of PpIX irradiation, resulting from the release of ROS [41], most DRG neurons survived the full 1200 s of laser exposure.

Using the whole-cell current-clamp recording configuration we examined the effects on membrane potential of ALA and irradiation either alone or in combination (Fig. 2D). DRG neurons exhibited infrequent spontaneous action potentials under control conditions. Neither ALA treatment (-57 ± 3 mV, n = 7) nor laser irradiation alone (-60 ± 3 mV, n = 5) affected the resting membrane potential or frequency of spontaneous action potentials (Fig. 2D). However, laser irradiation of DRG neurons treated with ALA (4-7 h) led to a sustained depolarisation (of 9 ± 1 mV, n = 3) and the appearance of frequent action potentials (Fig. 2D).
Taken together, these *in vitro* data demonstrate that neither PpIX production nor laser irradiation alone is sufficient to generate action potentials in nociceptive neurons. However, a combination of the two leads to depolarization of neurons initiating bursts of action potentials.

3.5. Singlet O_2 participates in phototoxicity-evoked excitation of DRG neurons

We investigated the possible involvement of ROS in the activation of nociceptive neurons using L-tryptophan, an antioxidant that prevents cell death induced by PpIX irradiation by scavenging singlet O_2 and tempol, a superoxide scavenger [32]. Incubation of ALA-treated DRG neuron cultures in the presence of L-tryptophan (2 mM) significantly increased ($p = 0.021$; t-test) the light dose required for the initiation of action potentials from 39 ± 6 J/cm^2 (n = 9) to 67 ± 9 J/cm^2 (n = 8) by PpIX irradiation, without significantly affecting the frequency of action potentials (Fig. 3A). By contrast, tempol (1 mM) had no effect on either parameter. These data reveal an involvement of singlet O_2 in the phototoxicity-evoked excitation of DRG neurons.

3.6. Proliferating cells initiate PpIX phototoxicity-evoked action potentials in DRG neurons

The activation of nociceptive neurons by PpIX irradiation could be caused directly by singlet O_2 generated within the neuron or through the release of mediators from adjacent glial cells. We took advantage of the relative scarcity of glial cells in the vicinity of DRG neurons on days 1 and 2 *in vitro* to investigate whether their presence influences the activation of action potentials by PpIX phototoxicity (Supplemental Fig. 3). Most neurons begin to respond to PpIX irradiation on day 3 *in vitro*, in keeping with a requirement for proliferating non-neuronal cells. The mean light dose required to activate the first burst of action potentials decreased from day 3. We performed a one-way ANOVA to compare the light dose required to trigger the first burst of action potentials with the number of days in culture ($F_{10,153} = 5.0$; $p < 0.0001$). A *post-hoc* Dunnett's comparison revealed a significant reduction in light dose from day 5 (all $p < 0.0001$ vs Day 2; Fig. 3B). Action potential frequency (Fig. 3C) and the proportion of cells exhibiting bursts of action potentials (Fig. 3D) increased from day 3. A one-way ANOVA revealed significant changes in action potential frequency with the number of days in culture ($F_{11,161} = 2.8$; $p = 0.002$). The increase in action potential frequency reached statistical significance *post-hoc* Dunnett's comparison vs Day 1) on days 6 ($p = 0.044$), 7 ($p = 0.013$) and 9 ($p = 0.007$; Fig. 3C). This coincides with the proliferation of non-neuronal cells (Supplemental Fig. 3).

We further explored a role for proliferating non-neuronal cells using transformed human keratinocyte (HaCaT) skin cells [7]. Exposure of HaCaT cells to ALA caused the production of PpIX as evidenced by fluorescence emission (Supplemental Fig. 4A). Laser irradiation following exposure to ALA led to substantial cell death (Supplemental Fig. 4B). We investigated whether growing DRG neurons on HaCaT cells influences the activation of nociceptors by PpIX irradiation.

The light dose required to activate the first burst of DRG action potentials following irradiation was dramatically decreased by the presence of HaCaT cells (Fig. 3E). The latency to the first burst significantly decreased ($p < 0.0001$; t-test) from 778 ± 121 s (n = 5) in the absence to 63 ± 22 s (n = 9) in the presence of HaCaT cells. This corresponds to a significant reduction ($p < 0.0001$; t-test) in the threshold light dose required to produce action potentials in nociceptive neurons from 75 ± 12 J/cm^2 to 6 ± 2 J/cm^2 (Fig. 3E). By contrast, the frequency of neuronal firing was unaffected by HaCaT cells (data not shown). Taken together, these data suggest that PpIX irradiation-evoked excitation of DRG neurons requires the generation of ROS by proliferating cells.

3.7. TRPV1 Inhibition suppresses PpIX phototoxicity-evoked action potentials

The *in vivo* data suggest that PpIX irradiation causes thermal hyperalgesia (Fig. 1F). This observation, together with patient reports that PpIX mediated pain resembles a burning sensation, implicates the involvement of the heat activated ion channel TRPV1 a mediator of thermal pain on primary afferent nociceptors [19,27,28,38]. Indeed, a recent study demonstrated that both ion channels are activated by PDT with blue light [1]. We examined the effect of AMG-9810 (1 and 3 μM), a selective TRPV1 antagonist [26], on phototoxicity-evoked action potentials initiated by irradiation with red light. AMG-9810 caused a concentration-dependent inhibition of action potentials, with 3 μM AMG-9810 significantly ($p = 0.001$; t-test) reducing the frequency of action potentials (Fig. 4A).

We explored the selectivity of AMG-9810 (1 μM) by applying the antagonist to either TRPV1 or TRPA1 receptors, while recording currents evoked by capsaicin (1 μM) and carvacrol (100 μM), respectively. AMG-9810 inhibited currents mediated by both TRPV1 (45 ± 5% inhibition, n = 3) and TRPA1 (22 ± 12% inhibition, n = 5) receptors (Fig. 4B). Next we used the same approach to explore the selectivity of the TRPA1 antagonist, HC-030031. HC-030031 (10 μM) blocked currents mediated by TRPA1 (89 ± 5% inhibition, n = 3), but had no effect on currents mediated by TRPV1 receptors (2 ± 1% inhibition, n = 4; Fig. 4C). Therefore we used HC-030031 to determine whether there is a role for TRPA1 in phototoxicity-evoked action potentials. HC-030031 (10 μM) had no significant effect on either the threshold light dose ($p = 0.2$) or action potential frequency ($p = 0.5$; Fig. 4D).

Taken together, the data implicate the involvement of TRPV1 receptor activity in PDT-mediated DRG activation.

3.8. Heat is not responsible for PpIX phototoxicity-evoked TRPV1 activity

TRPV1 channels on primary nociceptive neurons integrate diverse signals including noxious heat, inflammatory mediators and lipid metabolites [26]. These mediators of pain can activate TRPV1 channels in their own right and/or modulate thermal activation. TRPV1 channels have a thermal activation threshold of >40^{o}C which falls in the presence of inflammatory mediators and other sensitizers [26,31]. We explored whether heat may play a role in the PpIX irradiation-evoked excitation of nociceptive neurons. An irradiation light dose of 115 J/cm^2, equivalent to the maximum exposure of DRG neurons, caused only a 1.3^{o}C temperature increase in the recording chamber (Fig. 5A). Furthermore, the use of a thermal imaging camera revealed that laser irradiation (3.7 J/cm^2) of SWISS mouse tails elevated temperature by < 2^{o}C (Fig. 5B). Neither the *in vivo* nor the *in vitro* temperature increase is sufficient to reach the thermal threshold of TRPV1 activation [9]. This presumably explains why laser irradiation alone fails to initiate either pain (Fig. 1A) or action potentials (Fig. 2B - D). However, PpIX irradiation may cause the release of thermal sensitizers and/or direct activators of TRPV1 channels on nociceptive neurons.

Bradykinin is a known sensitizer of TRPV1 channels to heat through activation of bradykinin B2 receptors [26]. The B2 antagonist HOE140 (1 µM, n = 15) had no effect on PpIX phototoxicity-evoked action potentials recorded from DRG neurons (Fig. 5C). These data suggest that B2 receptor activation is not required for thermal sensitization of TRPV1 channels during PpIX-phototoxicity.

3.9. Evidence for an involvement of lipid metabolites in PpIX irradiation-evoked action potentials

We next examined whether there is a role for lipid metabolites in PpIX irradiation-evoked excitation of DRG neurons. N-arachidonoyl serotonin (AA-5-HT) inhibits fatty acid amide hydrolase (FAAH) when applied at µM concentrations, thereby reducing production of endogenous lipid metabolites that may activate and/or sensitize TRPV1 channels [6,24]. Furthermore, when applied at nM concentrations, AA-5-HT has been reported to inhibit intracellular Ca^{2+} increases caused by capsaicin-evoked activation of recombinant TRPV1 receptors [24]. AA-5-HT (100 nM) had no significant effect on the threshold light dose, or the frequency of PpIX sensitivity-evoked action potentials when applied to DRG neurons (n = 5; data not shown). However, a higher concentration of AA-5-HT (1 µM; n = 8) significantly inhibited action potential frequency ($p = 0.031$; t-test), without affecting the light dose required to initiate

the first burst of action potentials (Fig. 5D). Furthermore, AA-5-HT (1 μM) failed to inhibit currents mediated by recombinant rodent TRPV1 channels recorded from outside-out patches excised from HEK cells (n = 4; Fig. 5E) demonstrating that AA-5-HT (1 μM) is inactive at TRPV1 channels. We also tested the selective FAAH antagonist, PF-3845 (2 μM; n = 12) which, like AA-5-HT, significantly inhibited action potential frequency ($p = 0.004$; t-test), without affecting the threshold light dose (Fig. 5D). Taken together the data suggest that FAAH metabolites liberated by PpIX irradiation activate TRPV1 channels leading to excitation of action potentials in DRG neurons.

3.10. Local anaesthetic suppression of PpIX phototoxicity-evoked action potentials

Nerve blockade by local anaesthetics inhibits pain associated with PDT [38]. We examined whether lidocaine affects PpIX phototoxicity-evoked action potentials in DRG neurons. Lidocaine (100 μM; n = 5) inhibited action potential frequency ($p = 0.04$; t-test) without significantly affecting the threshold light dose (Fig. 6A). Lidocaine also reduced the percentage of cells that responded to PDT from 100% to 60%.

QX-314 is a positively charged quaternary lidocaine derivative that is unable to cross the DRG cell membrane directly and does not affect voltage-activated Na^+ channels when applied extracellularly, but can gain access to the inside of cells through open TRPV1 or TRPA1 channels [5,8]. Consistent with this, when applied concomitantly QX-314 (5 mM) inhibited action potentials evoked by capsaicin (30 μM; Fig. 6B). QX-314 (5 mM; n = 9), applied to the recording chamber, also significantly ($p < 0.0001$; t-test) inhibited PpIX irradiation-evoked action potential frequency without affecting the threshold light dose (Fig. 6C) and reduced the percentage of cells that responded to PDT from 100% to 67%. Since TRPA1 receptors do not participate in phototoxicity-evoked action potentials (Fig. 4D), these data support the hypothesis that TRPV1 channels enable intracellular access of QX-314. However, we cannot rule out the possibility of an alternative route of QX-314 entry [8].

3.11. Menthol suppresses PpIX phototoxicity-evoked action potentials and pain

Menthol causes a cooling sensation by activating TRPM8 receptors and also exhibits local anaesthetic effects through inhibition of voltage-activated Na^+ channels on nociceptive neurons [30]. We examined whether menthol (300 μM and 600 μM) inhibits PpIX irradiation-evoked action potentials recorded from DRG neurons. Menthol inhibited action potential frequency in a

concentration-dependent manner (Fig. 7A). There was a statistically significant reduction of action potential frequency (with respect to control) at 600 μM ($p < 0.035$; t-test). Also, the percentage of cells that responded to PDT was reduced by menthol (600 μM) from 100% to 33%. Menthol (300 μM) had no effect on the threshold light dose; however, the reduction in the number of cells responding in the presence of 600 μM menthol precluded analysis of the average threshold light dose in this case.

We next investigated whether menthol affects PpIX phototoxicity-evoked pain behavior in mice. The application of menthol (16%) in aqueous cream had no effect on PpIX-mediated fluorescence determined using the photospectrometer with fibre-optic coupled laser excitation at 405 nm (Fig. 7B). The application of menthol (2% and 16%) to the tails of SWISS mice 600 s prior to laser (630 nm, 3.7 J/cm^2) irradiation caused a dose-dependent reduction in the duration of pain behaviour (Fig. 7C). Vehicle treated mice did not respond to irradiation with pain behaviour (0.3 ± 0.3 s; n = 15), while ALA treated mice treated with aqueous cream 600 s prior to laser irradiation exhibited pain behaviour (28 ± 4 s; n = 15; Fig. 7C), consistent with our prior observations (Fig. 1A). By contrast, ALA treated mice receiving 2% or 16% menthol displayed pain behaviour lasting 11 ± 3 s (n = 10) and 8 ± 2 s (n = 10), respectively. A one-way ANOVA revealed a significant ($F_{3,46} = 22.9$; $p < 0.0001$) difference in mean pain behaviour duration (Fig. 7C). A *post-hoc* Dunnett's comparison (vs ALA treated mice receiving aqueous cream vehicle) demonstrated a significant reduction in pain behaviour in mice receiving 2% or 16% menthol (both $P < 0.0001$). These data suggest that menthol is an effective analgesic for treating PpIX irradiation-evoked pain.

Discussion

Pain caused by drug-induced phototoxicity is a widely encountered problem in clinical medicine. Accumulation of PpIX is a leading cause of phototoxicity resulting in acute pain during light exposure both in individuals suffering from the most common inherited cutaneous porphyria, EPP, and in most patients receiving PDT to treat skin diseases, such as skin cancers and pre-cancers [19,27,28,38]. Approximately 20% of the UK population aged ≥ 60 is affected by AK [17,25] and we estimate that ~33% may benefit from PDT. Furthermore, in Caucasians, BCC is the most common cancer; with ~110,000 UK adults developing the disease each year [34]. Similarly, around a third may benefit from PDT. Cutaneous porphyrias are less common (in Scotland ~ 1 in 10,000 and only 7.6 in 100,000 being EPP [11]). Nevertheless, porphyrias have a major health impact, with lifelong symptoms. Thus, porphyrin-induced pain represents a significant unmet clinical need.

We developed an *in vivo* mouse behavioral model of pain evoked by PpIX phototoxicity initiated by 630 nm light and investigated its molecular mechanisms *in vitro* using cultured primary afferent DRG neurons. Using these approaches we examined the underlying molecular mechanisms and identified menthol as a topical analgesic, which may be effective in the treatment of pain associated with PpIX-induced phototoxicity.

PpIX phototoxicity-induced pain behavior in mice was characterised by tail lifting, holding and licking following light exposure. The highly pigmented tails of C57 mice exhibited lower PpIX-mediated fluorescence and there was less pain behaviour than was observed with SWISS mice that lacked pigmentation. By contrast, the level of PpIX fluorescence in the less pigmented paw skin was similar in white and black mice demonstrating that there was no difference in the abilities of the two mouse strains to synthesize PpIX in response to topical ALA. Instead, skin pigmentation absorbs the irradiation required to elicit PpIX excitation. Indeed, α-melanocyte-stimulating hormone and similar drugs that cause melanin accumulation reduce the photosensitivity of patients with cutaneous porphyrias [16,36].

PpIX phototoxicity in SWISS mice also caused thermal hyperalgesia as evidenced by a reduction in tail withdrawal latency from hot water compared to mice that received either laser or photosensitizer alone. A heightened thermal response could be caused by PpIX phototoxicity-evoked activation of TRPV1 channels on primary afferent nociceptive DRG neurons. Consistent

with this, PpIX phototoxicity induced action potentials in cultured DRG neurons, which were reduced in frequency to negligible levels by the TRPV1 antagonist AMG-9810 or extracellular application of the quaternary lidocaine derivative QX-314. Extracellular QX-314 can enter nociceptive neurons expressing active TRPV1 channels causing blockade of their voltage-activated Na^+ channels [5]. By contrast to the blockade by the TRPV1 antagonist, the TRPA1 antagonist HC-030031 had no effect on action potential frequency. This suggests that action potentials evoked by PpIX phototoxicity during irradiation by 630 nm light is mediated through TRPV1 and not TRPA1 receptors.

TRPV1 channels can be activated by a variety of stimuli including noxious heat [9,26,40]. However, the temperature of both the mouse tail and the recording chamber during *in vivo* and *in vitro* laser exposure, respectively, remained well below the threshold for TRPV1 activation. Therefore it is unlikely that 630-nm irradiation provides a thermal stimulus for TRPV1 activation. In keeping with this, red light alone neither caused acute pain behavior nor thermal hypersensitivity. Inflammatory mediators, such as bradykinin, sensitize TRPV1 channels, reducing their thermal activation threshold [9,26]. However, the bradykinin receptor antagonist, HOE140, did not affect PpIX evoked action potentials in DRG neurons suggesting that bradykinin is not involved.

Lipid metabolites also play a role in TRPV1 channel activation and sensitization to heat pain [31]. Furthermore, FAAH inhibitors, which inhibit the metabolism of the endocannabinoid, anandamide, to arachidonic acid, are analgesic [10]. In keeping with a role for fatty acid metabolites downstream of FAAH in PpIX phototoxicity pain triggered by red light, the FAAH inhibitor, AA-5-HT, reduced action potential frequency in DRG neurons. AA-5-HT did not directly antagonise recombinant rodent TRPV1 receptors, implying that its inhibition of PpIX-evoked action potentials is mediated through altered lipid metabolism. In support of this hypothesis the selective FAAH antagonist, PF-3845, also inhibited action potentials. Several metabolites downstream of FAAH sensitize and/or activate TRPV1 channels including arachidonic acid, N-acyl-ethanolamines and prostaglandins [9,26]. These lipid metabolites are prime candidates as mediators of PpIX phototoxicity pain associated with red light. It is possible that FAAH antagonists might be of benefit for treating PDT pain. Additional experiments investigating whether FAAH antagonists reduce pain behaviour in mice will be important to explore this possibility.

Several lines of evidence suggest that the source of the lipid metabolite responsible for TRPV1 receptor activation is unlikely to be the DRG neuron itself. The threshold light dose required for PpIX-evoked action potentials was greatly diminished by an increased density of proliferating non-neuronal cells. This was most clearly demonstrated by co-culturing DRG neurons with human keratinocyte HaCaT cells, which dramatically reduced the threshold light dose for PpIX-evoked action potentials in DRG neurons. This suggests that the mediator of TRPV1 receptor activation is released from proliferating cells during PpIX phototoxicity. The demonstration that the $^1O_2$ scavenging antioxidant L-tryptophan increases the threshold light dose for PpIX-evoked action potentials suggests that ROS, generated by PpIX fluorescence in proliferating cells, trigger the release of a TRPV1 activator. The observation that the superoxide scavenger tempol had no effect on PpIX phototoxicity-evoked action potentials suggests that $^1O_2$, specifically, is implicated in the pain associated with PpIX-induced phototoxicity.

DRG neurons are remarkably resistant to PpIX phototoxicity due to high levels of singlet oxygen scavenging antioxidants [41], which likely limits both the availability of singlet oxygen and the autocrine generation of lipid metabolites. Instead, phototoxicity-evoked pain initiated by red light appears to require the paracrine action of lipid metabolites released from proliferating cells.

It is interesting that the excitatory response in whole cell recordings from DRG neurons was more sustained than that observed using the cell-attached configuration. A possible explanation for this could be desensitization of TRPV1 channels, which is known to be strongly influenced by Ca^{2+} accumulation [29]. It is possible that there is greater Ca^{2+} buffering capacity in the whole-cell configuration, by virtue of the electrode solution, which may limit TRPV1 desensitization. In future behavioral experiments it will be interesting to explore whether pain behaviour also exhibits desensitization.

The $^1O_2$ generated by PpIX phototoxicity directly affects lipids by reacting with *cis*-double bonds in unsaturated fatty acids including arachidonic acid [39] and this may lead to an increased production of additional TRPV1 active molecules. There are several oxidation products of arachidonic acid including 12(S)-hydroperoxyeicosatetraenoic acid, which is a TRPV1 agonist [9] and a possible participant in PpIX phototoxicity-evoked action potentials and pain.

A recent study demonstrated that blue light activates TRPV1 and TRPA1 channels, an effect that was enhanced by elevating PpIX levels [1]. The constitutive sensitivity of TRPA1 channels occurred over a range of wavelengths spanning UV_A and visible blue light. Not only was blue light capable of activating TRPA1 channels, blue light irradiation of human skin in the absence of a photosensitizer was associated with pain. By contrast, the application of a photosensitizer is a prerequisite for pain associated with red light exposure in patients [38]. Furthermore, our observations demonstrate the requirement for the application of a photosensitizer and irradiation to initiate action potentials in DRG neurons and pain behaviour in mice. It is interesting that phototoxicity evoked action potentials during irradiation by 630 nm light were resistant to the TRPA1 antagonist. This suggests that the causes of pain evoked by PDT with blue and red light may differ.

The *in vitro* and *in vivo* mouse models for PpIX-induced phototoxicity and pain provide approaches for identifying effective analgesic agents. We investigated menthol, which is commonly used for treating muscle pain. Recent studies suggest that menthol's analgesic actions are mediated through activation of TRPM8 channels, leading to the cooling sensation associated with menthol application, and through a local anaesthetic like state-dependent inhibition of voltage-activated Na^+ channels on DRG neurons [23,30]. Indeed, menthol suppressed PpIX-evoked action potentials in DRG neurons could be explained by direct inhibition of voltage-activated Na^+ channels. Topical menthol also reduced PpIX phototoxicity pain behavior in mice, without affecting PpIX photoactivation. In the whole animal the activation of TRPM8 receptors by menthol likely also contributes to analgesia by acting as a counterirritant and/or by engaging spinal gating mechanisms [33,42]. Experiments in TRPM8 knockout mice would help establish the role played by these receptors in the analgesic action of menthol on PDT pain. However, this will require refinement of the behavioral model of PDT pain to utilise a tissue that is less pigmented in C57 mice, such as the paw pad perhaps.

Regardless of its mode of action, based on our findings we anticipate that topical menthol will be effective for mitigating PpIX-induced pain and this will have important implications for optimisation of PDT treatment for patients with skin cancers and pre-cancers and for the management of patients with cutaneous porphyrias, notably erythropoietic protoporphyria. This will require further investigation in future clinical trials.

Acknowledgements

This work was supported by Tenovus Scotland (TGH) and a Wellcome Trust PhD Fellowship to (FB). We thank Dr Zhihong Huang and Fan Zhang for the infrared camera and assistance with the thermal imaging experiment, the Behavioural Neuroscience Core Facility for assistance with behavioural tests and Claire Sneddon for doing some of the dissections. We would also like to acknowledge the support of the Scottish PDT Centre for the provision of technical input and laser equipment. The authors declare that no conflict of interest exists.

Appendix A. Supplementary data

Figure Legends:

Figure 1. **PpIX-evoked pain behavior in mice**. A, Tail lifting, holding and licking in mice following laser irradiation (60 s, 3.7 J/cm^2). C57 and SWISS mouse tails were treated with vehicle soft white paraffin cream (vehicle) or cream containing ALA (20% w/w). ‡‡‡ indicates $p < 0.0001$. B, Spectroscopy analysis of *in vivo* PpIX fluorescence (arbitrary fluorescence units: AFU) in human forearm and the tails of SWISS mice either treated with vehicle or ALA. C, Peak PpIX fluorescence (FU) in the tails of C57 and SWISS mice treated with vehicle or ALA expressed as a percentage of the fluorescence in ALA-treated human forearm. ‡‡‡ indicates $p < 0.0001$. D, Peak fluorescence in the ears, tails and paws of C57 (black bars) and SWISS (gray bars) mice after topical ALA application to their tails. Application of black ink to ALA treated tails of SWISS mice abolished PpIX fluorescence (open bar). ** indicates $p = 0.006$, ††† indicates $p < 0.0001$. E, Graph of PpIX fluorescence (expressed as peak (634 nm) normalised to auto-fluorescence (500 nm); PF/AF) versus pain behavior reveals a lack of correlation. F, Graph of SWISS mouse tail withdrawal latencies from hot water (48^{o}C) after no treatment, vehicle cream, ALA, or ALA plus laser irradiation to tails. PpIX irradiation causes hypersensitivity evidenced by a reduction in tail withdrawal latency. † indicates $p = 0.029$. Statistics are expressed as * for t-tests, † for one-way ANOVA and ‡ for two-way ANOVA.

Figure 2. **PpIX irradiation evokes action potentials in primary afferent DRG neurons**. A, Confocal microscopy images of cells in DRG cultures on day 4 *in vitro*. Images represent fluorescence (top) and combined fluorescence/ bright field illumination (bottom). Exemplar DRG neurons are indicated by white arrows. Yellow arrows indicate cells that lack neuronal morphology. Graph shows flow cytometric analysis of cells in DRG cultures with (gray) and without (black) ALA. Inset graphs illustrate the regions of interest that define the cell populations used for gating. B, Cell-attached patch electrophysiological recording from DRG neurons from SWISS mice before and during laser irradiation. Cells received either no treatment (upper trace) or were treated with ALA (lower trace). C, Cell attached patch recordings from untreated (top trace) and ALA treated (bottom trace) C57 DRG neurons before and during laser irradiation. D, Whole-cell current clamp recordings from untreated (top trace) and ALA treated (bottom trace) C57 DRG neurons. In B - D horizontal lines indicate the period of laser irradiation and expanded traces depict the highest frequency action potentials recorded from these ALA treated cells during laser irradiation.

Figure 3. **Proliferating cells initiate PpIX irradiation evoked action potentials in DRG neurons**. A, Graph of DRG neuron action potential frequencies and threshold light doses (expressed as percent of control) after treatment with either L-tryptophan or tempol or in matched controls (culture days 6 and 7). * indicates p = 0.021. B, Graph of the light dose required to initiate action potentials in DRG neurons after 2 – 15 days in culture. ††† indicates p < 0.0001. C, Graph of action potential frequencies initiated by PpIX irradiation on day 1 – 15 in culture. Day 6 * indicates p = 0.044, Day 7 * indicates p = 0.013 and Day 9 ** indicates p = 0.007. D, Graph of the percentage of DRG neurons exhibiting action potentials during PpIX irradiation on day 1 – 15 in culture. E, An example of PpIX irradiation-evoked action potentials recorded on day 3 in culture from a neuron in the absence or in the presence of HaCaT cells (left panel). Right panel, average light dose required to initiate action potentials in ALA treated neurons on day 3 in the presence and absence of HaCaT cells. *** indicates P < 0.0001. Statistics are expressed as * for t-tests and † for one-way ANOVA.

Figure 4. **Inhibition of TRPV1-mediated excitation suppresses PpIX irradiation-evoked action potentials**. A, Graph of DRG neuron threshold light dose and action potential (AP) frequency (expressed as percent of control) after treatment with AMG-9810 (1 or 3 μM) or in matched controls (culture days 6 - 8). ** indicates p = 0.001, t-test. The absence of action potentials in the presence of 3 μM AMG-9810 prevented analysis of the threshold light dose. B, *Left*, Exemplar capsaicin (1 μM)-evoked current recorded from an outside-out patch excised from an HEK cell expressing TRPV1 receptors and, *right*, a whole-cell carvacrol (100 μM)-evoked current recorded from an HEK cell expressing TRPA1 receptors. AMG-9810 (3 μM) inhibited currents mediated by TRPV1 and TRPA1 receptors. C, By contrast, HC-030031 (10 μM) only inhibited carvacrol (100 μM)-evoked currents mediated by TRPA1 receptors, while capsaicin (1 μM)-evoked currents mediated by TRPV1 receptors were unaffected. D, Graph of DRG neuron threshold light dose and action potential (AP) frequency (expressed as percent of control) after treatment with HC-030031 (10 μM) or in matched controls (culture days 6 - 8).

Figure 5. **Inhibition of FAAH reduced the frequency of PpIX irradiation-evoked action potentials.** A, The temperature of saline (measured by a digital thermo-hygrometer) within the recording chamber increased by <1.5^{o}C during the 20 min laser (630 nM) irradiation. B, Likewise, infrared recording with a thermal imaging camera revealed that exposure of the mouse tail to laser irradiation for 60 s caused a temperature increase of <2^{o}C. C, Graph of action potential

frequencies and threshold light doses (expressed as percent of control) after treatment with the bradykinin B2 antagonist, HOE140 (1 μM), or in matched controls (culture days 6 and 7). D, Inhibition of fatty acid metabolism by the FAAH antagonists, AA-5-HT (1 μM) or PF-3845 (1 μM), reduced PpIX irradiation-evoked action potential frequency without affecting the threshold light dose. * indicates p = 0.031, ** indicates p = 0.004. E, An exemplar capsaicin (1 μM)-evoked current recorded from an outside-out patch excised from an HEK cell expressing TRPV1 receptors. The current was unaffected by co-application of AA-5-HT (1 μM). Statistics are expressed as single or double asterisks for t-tests.

Figure 6. **Suppression of PpIX irradiation-evoked action potentials by lidocaine and QX-314**. A, Lidocaine (100 μM) applied to the recording chamber inhibited PpIX irradiation evoked action potential frequency without significantly affecting the threshold light dose. * indicates p = 0.04. B, Action potentials evoked by local application of capsaicin (30 μM) were abolished by the co-application of QX-314 (5 mM) with partial reversal of block upon subsequent application of capsaicin alone. C, QX-314 (5 mM) inhibited PpIX irradiation evoked action potential frequency without affecting the threshold light dose. *** indicates p < 0.0001. Statistics are expressed as single or triple asterisks for t-tests.

Figure 7. **Menthol suppresses PpIX irradiation-evoked action potentials and pain**. A, Menthol (300 and 600 μM) caused a concentration-dependent inhibition of the frequency of PpIX irradiation-dependent action potentials. Menthol (300 μM) did not affect the threshold light dose. Menthol (600 μM) reduced the occurrence of action potentials to the extent that the threshold light dose could not be calculated. * indicates p = 0.035. B, Menthol (16% in aqueous cream) application to mouse tails did not affect ALA induced PpIX fluorescence (FU) detected by laser diode spectroscopy, expressed as a percentage of the ALA-induced PpIX fluorescence in human forearm. C, A bar graph of PpIX irradiation-evoked pain behaviour when mouse tails were treated with vehicle or with ALA. Mouse tails treated with ALA were treated with vehicle, 2% menthol or 16% menthol. ††† indicates p < 0.0001. Statistics are expressed as * for t-tests and † for one-way ANOVA.

References

[1] Babes A, Sauer SK, Moparthi L, Kichko TI, Neacsu C, Namer B, Filipovic M, Zygmunt PM, Reeh PW, Fischer MJ. Photosensitization in Porphyrias and Photodynamic Therapy Involves TRPA1 and TRPV1. J Neurosci 2016;36(19):5264-5278.

[2] Balwani M, Doheny D, Bishop DF, Nazarenko I, Yasuda M, Dailey HA, Anderson KE, Bissell DM, Bloomer J, Bonkovsky HL, Phillips JD, Liu L, Desnick RJ, Porphyrias Consortium of the National Institutes of Health Rare Diseases Clinical Research N. Loss-of-function ferrochelatase and gain-of-function erythroid-specific 5-aminolevulinate synthase mutations causing erythropoietic protoporphyria and x-linked protoporphyria in North American patients reveal novel mutations and a high prevalence of X-linked protoporphyria. Mol Med 2013;19:26-35.

[3] Baptista-Hon DT, Deeb TZ, Othman NA, Sharp D, Hales TG. The 5-HT3B subunit affects high-potency inhibition of 5-HT3 receptors by morphine. Br J Pharmacol 2012;165(3):693-704.

[4] Bautista DM, Siemens J, Glazer JM, Tsuruda PR, Basbaum AI, Stucky CL, Jordt SE, Julius D. The menthol receptor TRPM8 is the principal detector of environmental cold. Nature 2007;448(7150):204-208.

[5] Binshtok AM, Bean BP, Woolf CJ. Inhibition of nociceptors by TRPV1-mediated entry of impermeant sodium channel blockers. Nature 2007;449(7162):607-610.

[6] Bisogno T, Melck D, De Petrocellis L, Bobrov M, Gretskaya NM, Bezuglov VV, Sitachitta N, Gerwick WH, Di Marzo V. Arachidonoylserotonin and other novel inhibitors of fatty acid amide hydrolase. Biochem Biophys Res Commun 1998;248(3):515-522.

[7] Boukamp P, Petrussevska RT, Breitkreutz D, Hornung J, Markham A, Fusenig NE. Normal keratinization in a spontaneously immortalized aneuploid human keratinocyte cell line. J Cell Biol 1988;106(3):761-771.

[8] Brenneis C, Kistner K, Puopolo M, Jo S, Roberson D, Sisignano M, Segal D, Cobos EJ, Wainger BJ, Labocha S, Ferreiros N, von Hehn C, Tran J, Geisslinger G, Reeh PW, Bean BP, Woolf CJ. Bupivacaine-induced cellular entry of QX-314 and its contribution to differential nerve block. Br J Pharmacol 2014;171(2):438-451.

[9] Cao E, Cordero-Morales JF, Liu B, Qin F, Julius D. TRPV1 channels are intrinsically heat sensitive and negatively regulated by phosphoinositide lipids. Neuron 2013;77(4):667-679.

[10] Clapper JR, Moreno-Sanz G, Russo R, Guijarro A, Vacondio F, Duranti A, Tontini A, Sanchini S, Sciolino NR, Spradley JM, Hohmann AG, Calignano A, Mor M, Tarzia G, Piomelli D. Anandamide suppresses pain initiation through a peripheral endocannabinoid mechanism. Nat Neurosci 2010;13(10):1265-1270.

[11] Dawe RS. Prevalences of chronic photodermatoses in Scotland. Photodermatol Photoimmunol Photomed 2009;25(1):59-60.

[12] DeRosa MC, Crutchley RJ. Photosensitized singlet oxygen and its applications. Coordination Chemistry Reviews 2002;233:351-371.

[13] Ducamp S, Schneider-Yin X, de Rooij F, Clayton J, Fratz EJ, Rudd A, Ostapowicz G, Varigos G, Lefebvre T, Deybach JC, Gouya L, Wilson P, Ferreira GC, Minder EI, Puy H. Molecular and functional analysis of the C-terminal region of human erythroid-specific 5-aminolevulinic synthase associated with X-linked dominant protoporphyria (XLDPP). Hum Mol Genet 2013;22(7):1280-1288.

[14] Ericson MB, Wennberg AM, Larko O. Review of photodynamic therapy in actinic keratosis and basal cell carcinoma. Ther Clin Risk Manag 2008;4(1):1-9.

[15] Hales TG, Sanderson MJ, Charles AC. GABA has excitatory actions on GnRH-secreting immortalized hypothalamic (GT1-7) neurons. Neuroendocrinology 1994;59(3):297-308.

[16] Harms J, Lautenschlager S, Minder CE, Minder EI. An alpha-melanocyte-stimulating hormone analogue in erythropoietic protoporphyria. N Engl J Med 2009;360(3):306-307.

[17] Harvey I, Frankel S, Marks R, Shalom D, Nolan-Farrell M. Non-melanoma skin cancer and solar keratoses. I. Methods and descriptive results of the South Wales Skin Cancer Study. Br J Cancer 1996;74(8):1302-1307.

[18] Horner ME, Alikhan A, Tintle S, Tortorelli S, Davis DM, Hand JL. Cutaneous porphyrias part I: epidemiology, pathogenesis, presentation, diagnosis, and histopathology. Int J Dermatol 2013;52(12):1464-1480.

[19] Ibbotson SH. Adverse effects of topical photodynamic therapy. Photodermatol Photoimmunol Photomed 2011;27(3):116-130.

[20] Ibbotson SH, Jong C, Lesar A, Ferguson JS, Padgett M, O'Dwyer M, Barnetson R, Ferguson J. Characteristics of 5-aminolaevulinic acid-induced protoporphyrin IX fluorescence in human skin in vivo. Photodermatol Photoimmunol Photomed 2006;22(2):105-110.

[21] Klein AH, Sawyer CM, Carstens MI, Tsagareli MG, Tsiklauri N, Carstens E. Topical application of L-menthol induces heat analgesia, mechanical allodynia, and a biphasic effect on cold sensitivity in rats. Behav Brain Res 2010;212(2):179-186.

[22] Kochevar IE. Singlet oxygen signaling: from intimate to global. Sci STKE 2004;2004(221):pe7.

[23] Liu B, Fan L, Balakrishna S, Sui A, Morris JB, Jordt SE. TRPM8 is the principal mediator of menthol-induced analgesia of acute and inflammatory pain. Pain 2013;154(10):2169-2177.

[24] Maione S, De Petrocellis L, de Novellis V, Moriello AS, Petrosino S, Palazzo E, Rossi FS, Woodward DF, Di Marzo V. Analgesic actions of N-arachidonoyl-serotonin, a fatty acid amide hydrolase inhibitor with antagonistic activity at vanilloid TRPV1 receptors. Br J Pharmacol 2007;150(6):766-781.

[25] Memon AA, Tomenson JA, Bothwell J, Friedmann PS. Prevalence of solar damage and actinic keratosis in a Merseyside population. Br J Dermatol 2000;142(6):1154-1159.

[26] Morales-Lazaro SL, Simon SA, Rosenbaum T. The role of endogenous molecules in modulating pain through transient receptor potential vanilloid 1 (TRPV1). J Physiol 2013;591(Pt 13):3109-3121.

[27] Morton CA, Szeimies RM, Sidoroff A, Braathen LR. European guidelines for topical photodynamic therapy part 1: treatment delivery and current indications - actinic keratoses, Bowen's disease, basal cell carcinoma. J Eur Acad Dermatol Venereol 2013;27(5):536-544.

[28] Morton CA, Szeimies RM, Sidoroff A, Braathen LR. European guidelines for topical photodynamic therapy part 2: emerging indications--field cancerization, photorejuvenation and inflammatory/infective dermatoses. J Eur Acad Dermatol Venereol 2013;27(6):672-679.

[29] Numazaki M, Tominaga T, Takeuchi K, Murayama N, Toyooka H, Tominaga M. Structural determinant of TRPV1 desensitization interacts with calmodulin. Proc Natl Acad Sci U S A 2003;100(13):8002-8006.

[30] Pan R, Tian Y, Gao R, Li H, Zhao X, Barrett JE, Hu H. Central mechanisms of menthol-induced analgesia. J Pharmacol Exp Ther 2012;343(3):661-672.

[31] Patwardhan AM, Akopian AN, Ruparel NB, Diogenes A, Weintraub ST, Uhlson C, Murphy RC, Hargreaves KM. Heat generates oxidized linoleic acid metabolites that activate TRPV1 and produce pain in rodents. J Clin Invest 2010;120(5):1617-1626.

[32] Perotti C, Casas A, Del CBAM. Scavengers protection of cells against ALA-based photodynamic therapy-induced damage. Lasers Med Sci 2002;17(4):222-229.

[33] Proudfoot CJ, Garry EM, Cottrell DF, Rosie R, Anderson H, Robertson DC, Fleetwood-Walker SM, Mitchell R. Analgesia mediated by the TRPM8 cold receptor in chronic neuropathic pain. Curr Biol 2006;16(16):1591-1605.

[34] Reinau D, Surber C, Jick SS, Meier CR. Epidemiology of basal cell carcinoma in the United Kingdom: incidence, lifestyle factors, and comorbidities. Br J Cancer 2014;111(1):203-206.

[35] Serra-Guillen C, Hueso L, Nagore E, Vila M, Llombart B, Requena Caballero C, Botella-Estrada R, Sanmartin O, Alfaro-Rubio A, Guillen C. Comparative study between cold air analgesia and supraorbital and supratrochlear nerve block for the management of pain during photodynamic therapy for actinic keratoses of the frontotemporal zone. Br J Dermatol 2009;161(2):353-356.

[36] Tintle S, Alikhan A, Horner ME, Hand JL, Davis DM. Cutaneous porphyrias part II: treatment strategies. Int J Dermatol 2014;53(1):3-24.

[37] Walwyn W, Evans CJ, Hales TG. Beta-arrestin2 and c-Src regulate the constitutive activity and recycling of mu opioid receptors in dorsal root ganglion neurons. J Neurosci 2007;27(19):5092-5104.

[38] Warren CB, Karai LJ, Vidimos A, Maytin EV. Pain associated with aminolevulinic acid-photodynamic therapy of skin disease. J Am Acad Dermatol 2009;61(6):1033-1043.

[39] Watabe N, Ishida Y, Ochiai A, Tokuoka Y, Kawashima N. Oxidation decomposition of unsaturated fatty acids by singlet oxygen in phospholipid bilayer membranes. J Oleo Sci 2007;56(2):73-80.

[40] Wemmie JA, Taugher RJ, Kreple CJ. Acid-sensing ion channels in pain and disease. Nat Rev Neurosci 2013;14(7):461-471.

[41] Wright KE, MacRobert AJ, Phillips JB. Inhibition of specific cellular antioxidant pathways increases the sensitivity of neurons to meta-tetrahydroxyphenyl chlorin-mediated photodynamic therapy in a 3D co-culture model. Photochem Photobiol 2012;88(6):1539-1545.

[42] Zheng J, Lu Y, Perl ER. Inhibitory neurones of the spinal substantia gelatinosa mediate interaction of signals from primary afferents. J Physiol 2010;588(Pt 12):2065-2075.

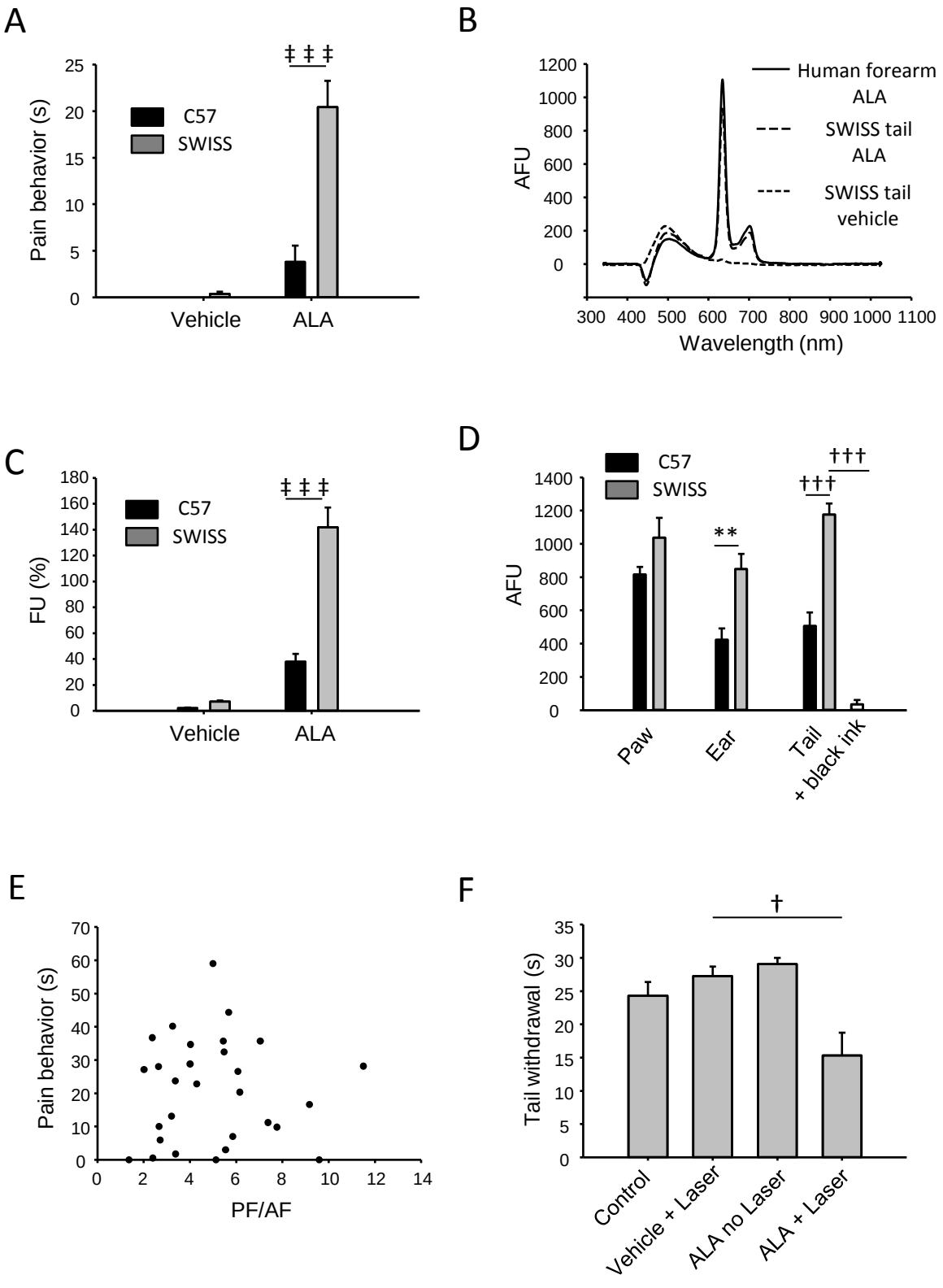
A
Pain behavior (s)
C57
SWISS
‡ ‡ ‡
Vehicle
ALA
B
AFU
Human forearm ALA
SWISS tail ALA
SWISS tail vehicle
Wavelength (nm)
C
FU (%)
C57
SWISS
‡ ‡ ‡
Vehicle
ALA
D
AFU
C57
SWISS
**
†††
†††
Paw
Ear
Tail + black ink
E
Pain behavior (s)
PF/AF
F
Tail withdrawal (s)
†
Control
Vehicle + Laser
ALA no Laser
ALA + Laser

A

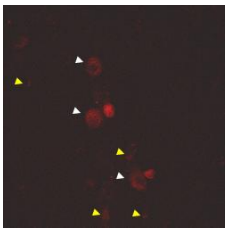

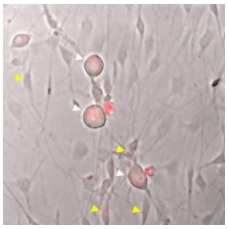

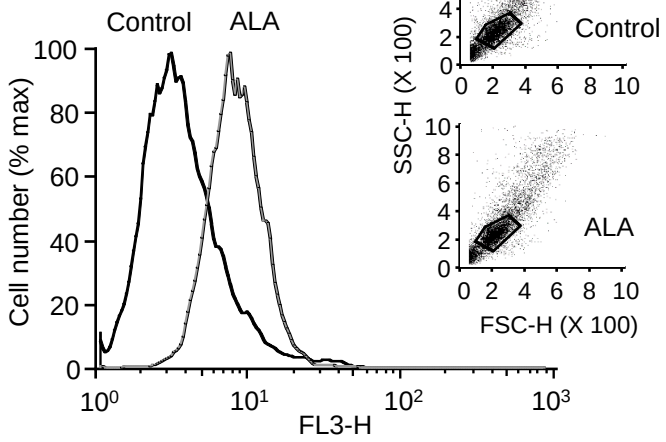
Control
ALA
Cell number (% max)
100
80
60
40
20
0
10^0
10^1
10^2
10^3
FL3-H
SSC-H (X 100)
FSC-H (X 100)
Control
ALA
0 2 4 6 8 10

B

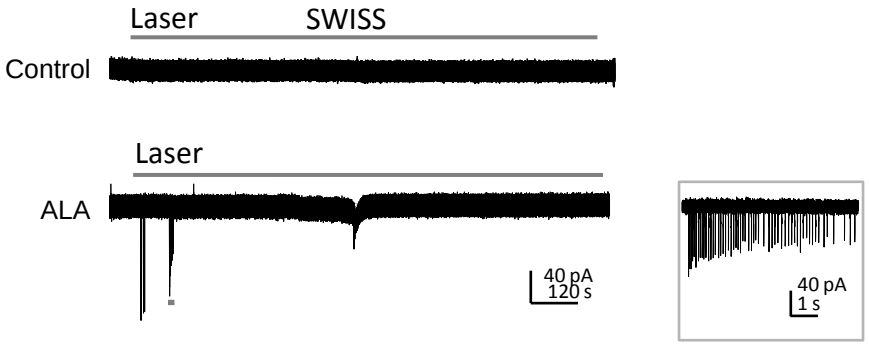
Laser
SWISS
Control
Laser
ALA
40 pA
120 s
40 pA
1 s

C

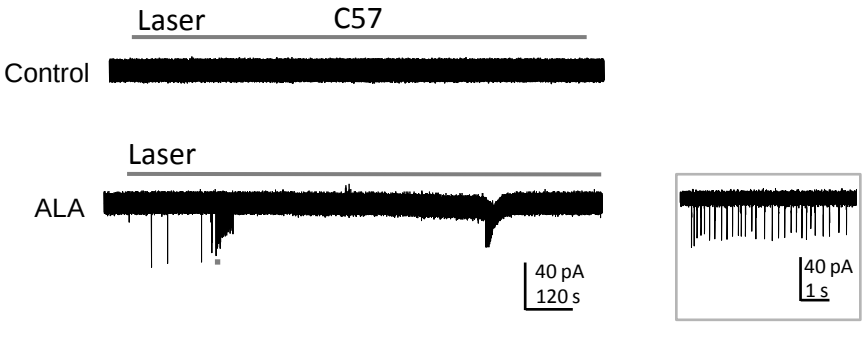
Laser
C57
Control
Laser
ALA
40 pA
120 s
40 pA
1 s

D

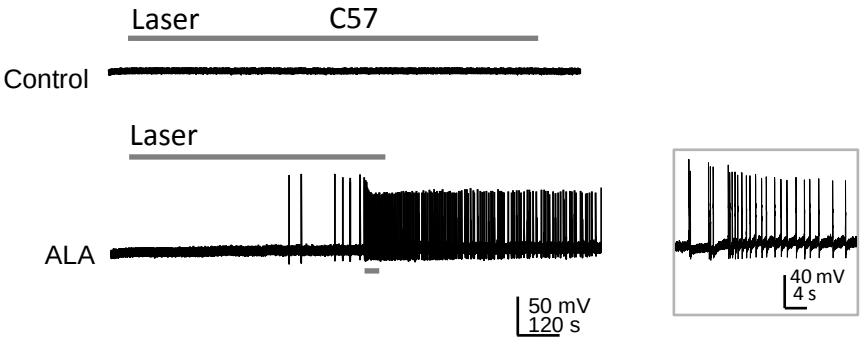
Laser
C57
Control
Laser
ALA
50 mV
120 s
40 mV
4 s

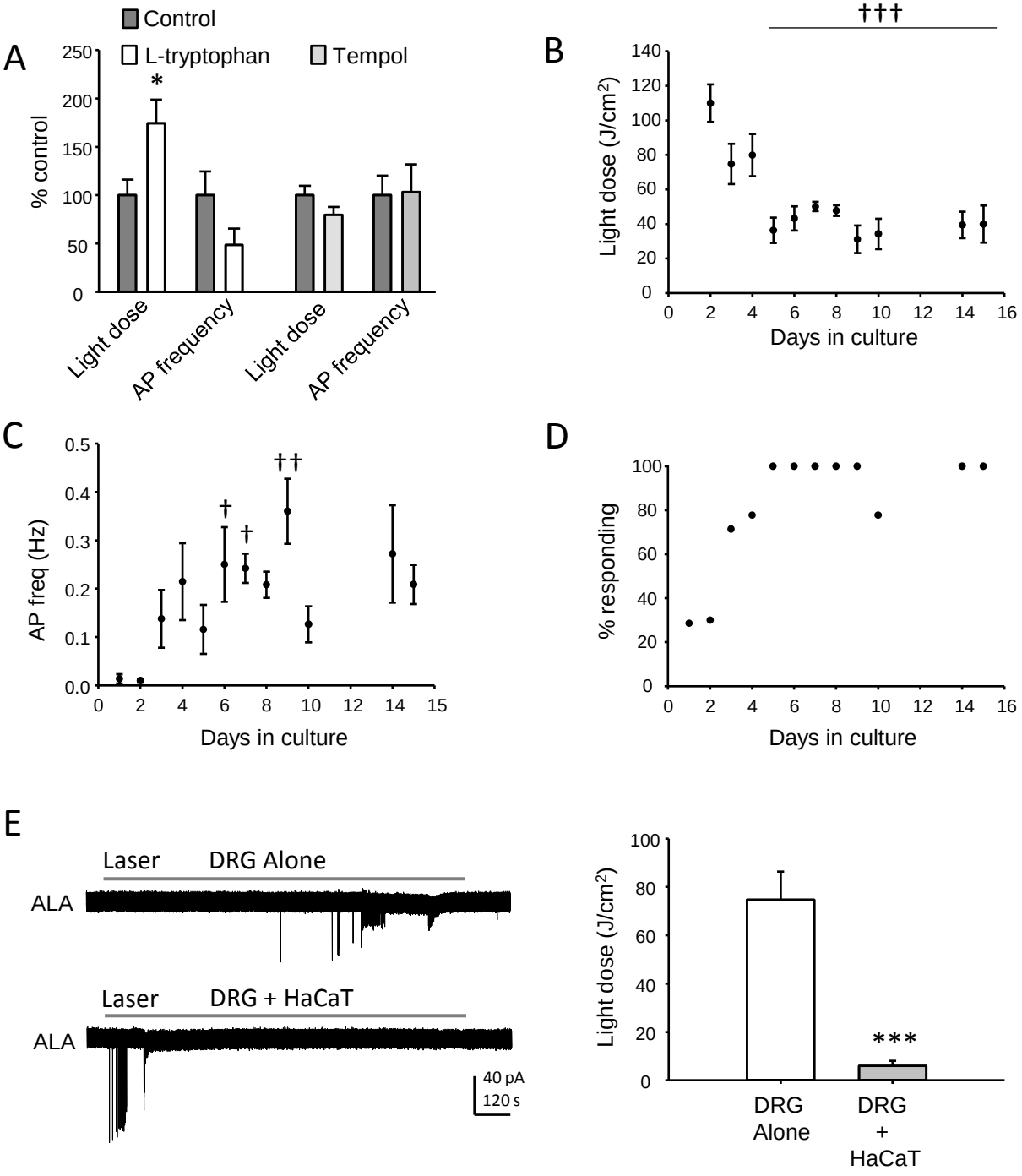
A
Control
L-tryptophan
Tempol
% control
Light dose
AP frequency
Light dose
AP frequency
B
Light dose (J/cm²)
Days in culture
C
AP freq (Hz)
Days in culture
D
% responding
Days in culture
E
Laser
DRG Alone
ALA
Laser
DRG + HaCaT
ALA
40 pA
120 s
Light dose (J/cm²)
DRG Alone
DRG + HaCaT

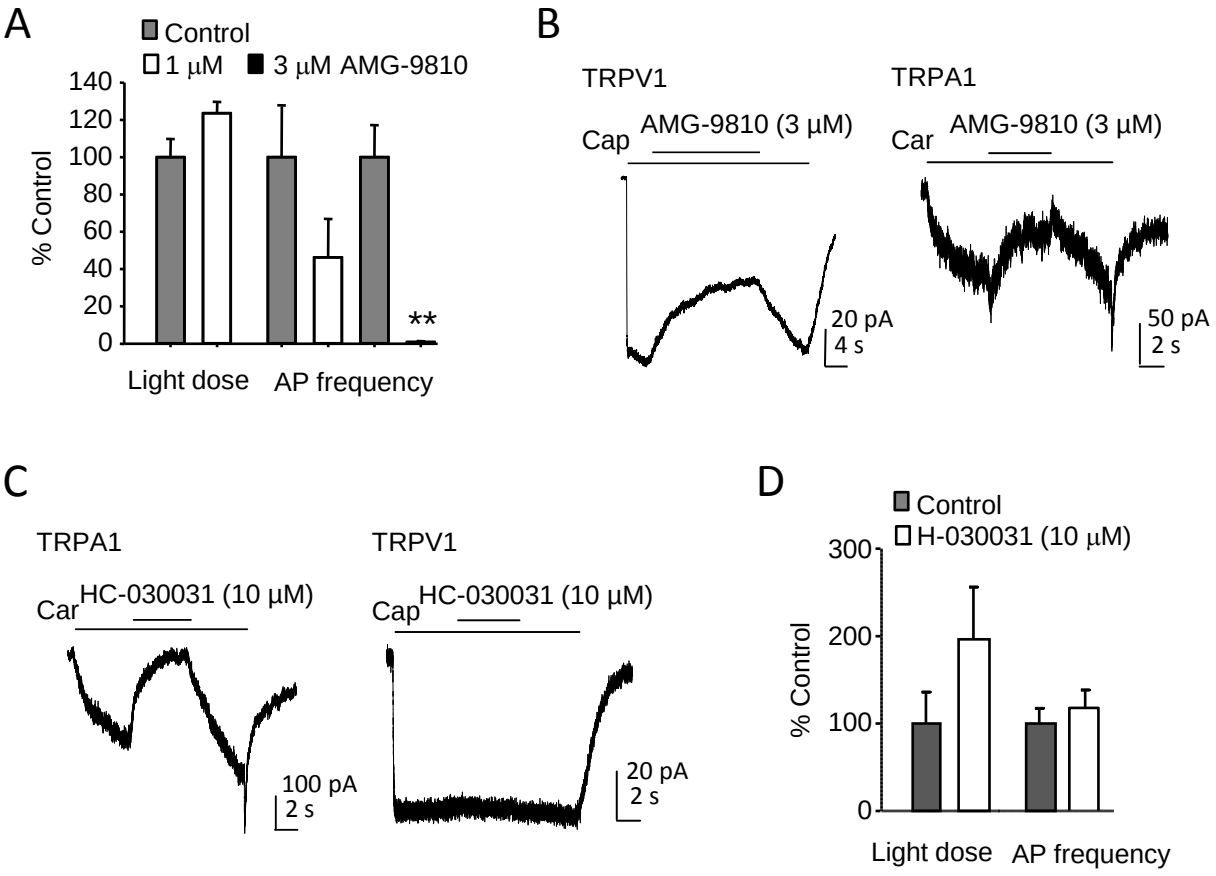
A
Control
1 μM
3 μM AMG-9810
% Control
140
120
100
80
60
40
20
0
**
Light dose
AP frequency
B
TRPV1
Cap
AMG-9810 (3 μM)
20 pA
4 s
TRPA1
Car
AMG-9810 (3 μM)
50 pA
2 s
C
TRPA1
Car
HC-030031 (10 μM)
100 pA
2 s
TRPV1
Cap
HC-030031 (10 μM)
20 pA
2 s
D
Control
H-030031 (10 μM)
% Control
300
200
100
0
Light dose
AP frequency

Fig. 5

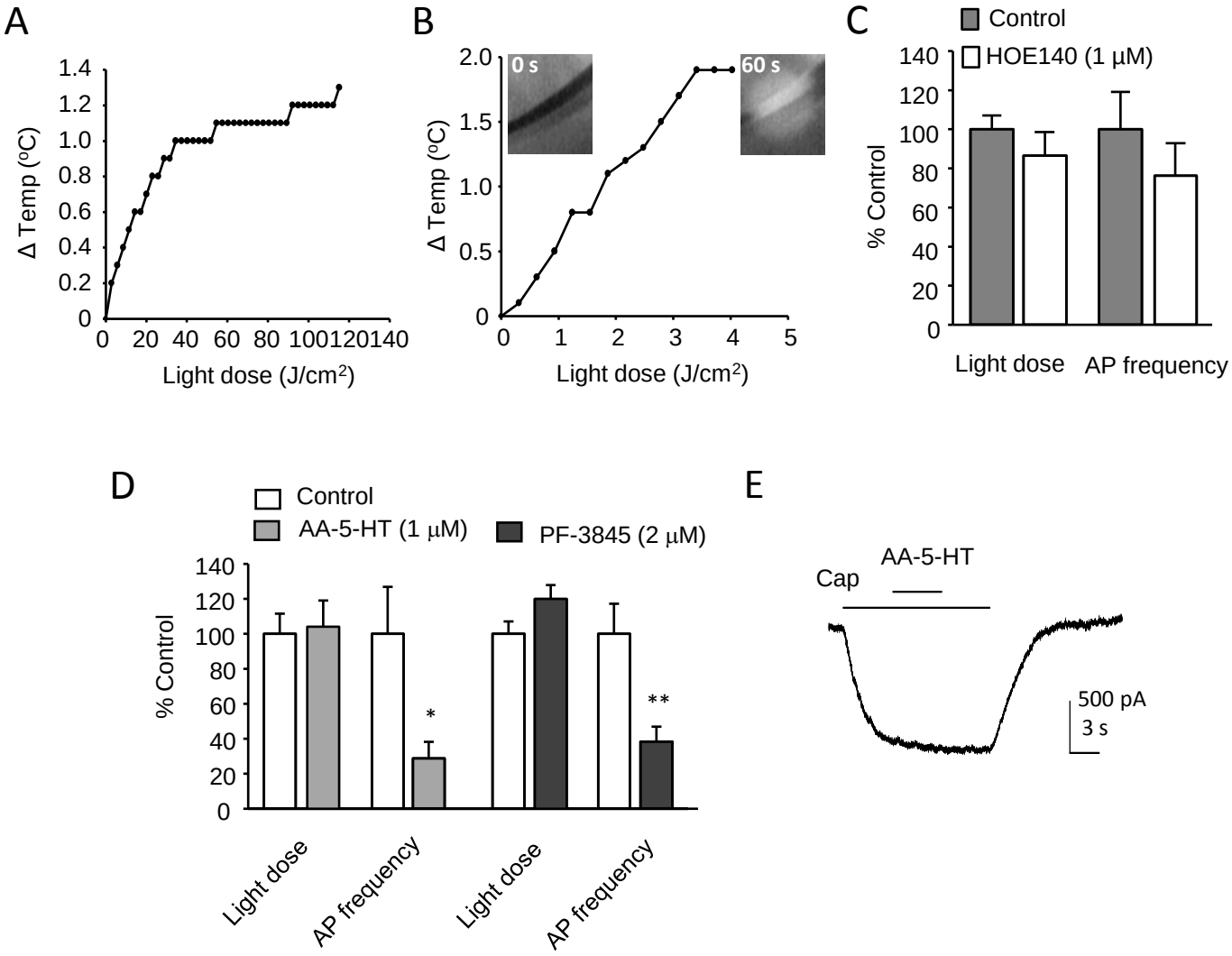
A
Δ Temp (°C)
Light dose (J/cm²)
B
0 s
60 s
Δ Temp (°C)
Light dose (J/cm²)
C
Control
HOE140 (1 μM)
% Control
Light dose
AP frequency
D
Control
AA-5-HT (1 μM)
PF-3845 (2 μM)
% Control
Light dose
AP frequency
Light dose
AP frequency
E
Cap
AA-5-HT
500 pA
3 s

Fig. 6

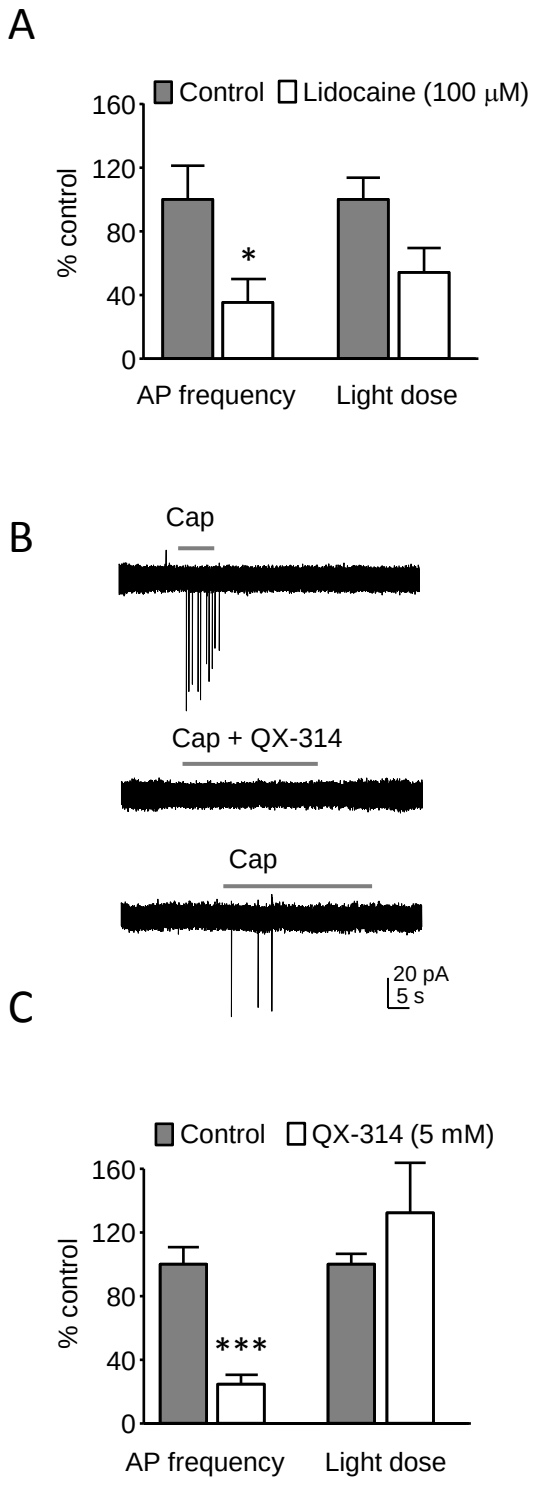
A
Control
Lidocaine (100 μM)
160
120
80
40
0
% control
*
AP frequency
Light dose
B
Cap
Cap + QX-314
Cap
20 pA
5 s
C
Control
QX-314 (5 mM)
160
120
80
40
0
% control
***
AP frequency
Light dose

A

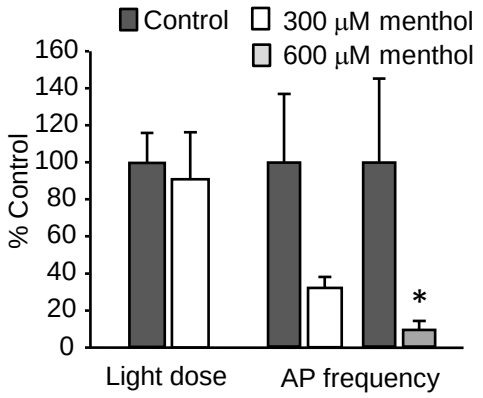
Control
300 μM menthol
600 μM menthol
% Control
160
140
120
100
80
60
40
20
0
*
Light dose
AP frequency

B

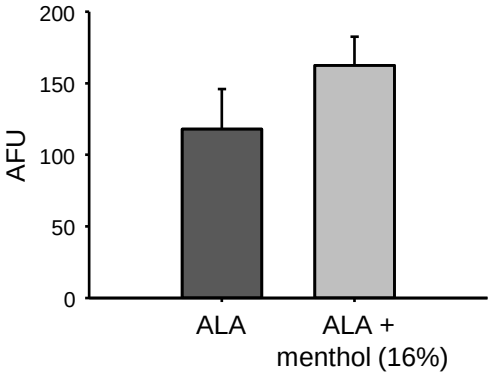
AFU
200
150
100
50
0
ALA
ALA +
menthol (16%)

C

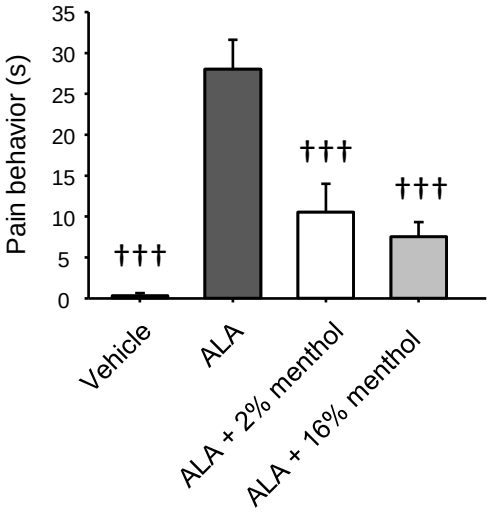
Pain behavior (s)
35
30
25
20
15
10
5
0
†††
†††
†††
Vehicle
ALA
ALA + 2% menthol
ALA + 16% menthol

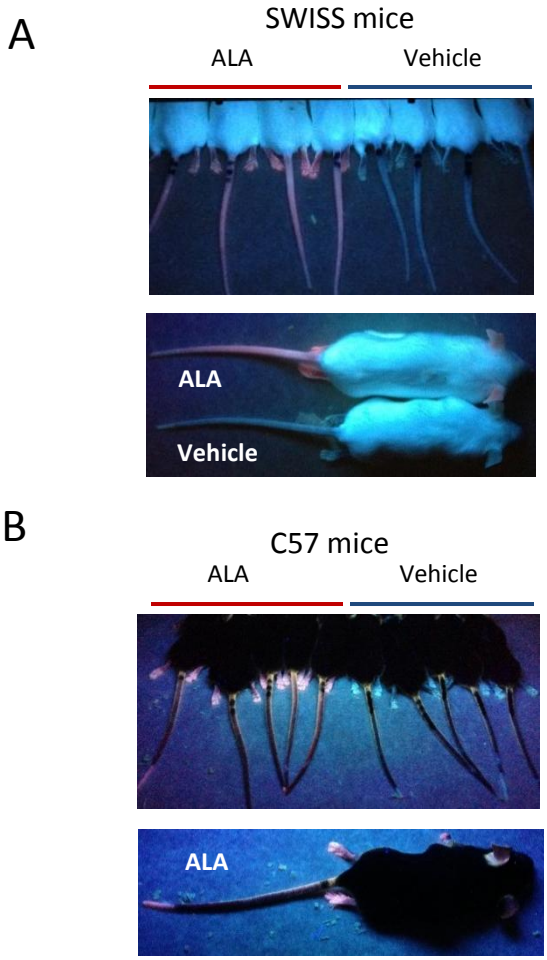

Fluorescence visualised using a Wood's lamp. A, top panel, SWISS white mice exhibited visible pink fluorescence in ALA treated tails, which was not evident in vehicle treated tails. Bottom panel, fluorescence was also visible in other tissues including paws, ears and noses. B, ALA treated C57 black mice exhibited visible fluorescence in skin that lacked dark pigmentation (particularly obvious and consistent in the paws).

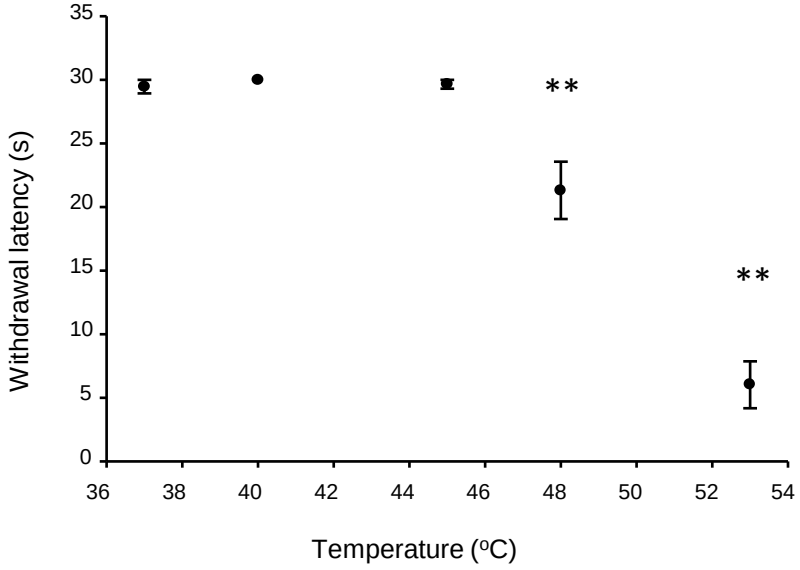

Tail withdrawal from heated water. The graph shows the relationship between SWISS mouse tail withdrawal latency as a percentage of the maximum time of exposure to heated water (30 s). Water at a temperature of 48°C (**P = 0.008) and 53oC (**P = 0.001) caused significant decreases in tail withdrawal latencies (One-sample Wilcoxon signed rank test vs 30 s).

Supplemental Fig. 3

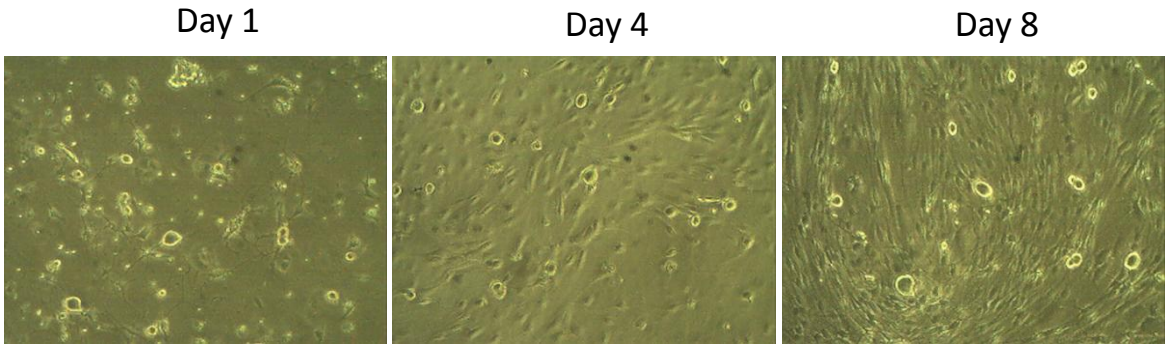

The number of supporting cells increase during DRG culture. Transmission microscopy reveals the proliferation of non-neuronal cells in DRG cultures in this case after four and eight days in vitro.

A

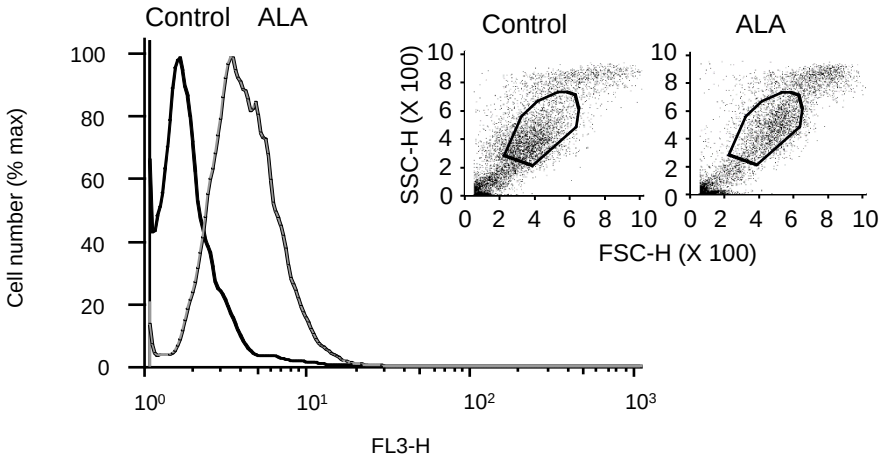

B

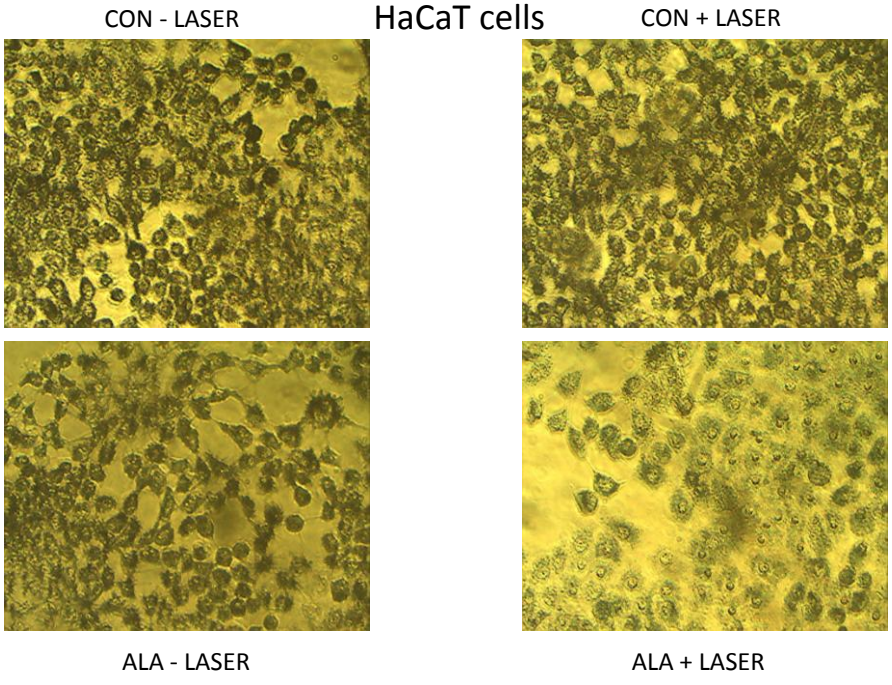

Non-neuronal cells are susceptible to phototoxicity. A, Flow cytometry analysis of HaCaT cells demonstrates fluorescence emission following treatment with ALA (1 mM for 4 h) that was not seen in control cells. B, The MTT (3-(4,5-dimethylthiazol-2-yl)-2,5-diphenyltetrazolium bromide) assay was used to detect viable ALA treated HaCat cells (darkly stained) before and after irradiation (630 nm, with an irradiance of 96 mW/cm^2). ALA treated HaCaT keratinocyte cells exhibit substantial cell death (fewer darkly stained cells) after a similar exposure to irradiation.